

TEXTURE ANALYSIS OF MAGNETIC RESONANCE T1 MAPS AND EXTRACELLULAR VOLUME IN HEART FAILURE COMPARED WITH NORMAL CONTROLS

Chau Thi Ngoc Anh¹, Ming - Ting Wu²

SUMMARY

Objective: To assess the T1 and extracellular volume (ECV) maps of left ventricle (LV) of patients with non-ischemic heart failure (NIHF) by cardiac MRI

Materials & Methods: This retrospective study included 23 NIHF (mean age = 48.1 years, 12 M), 25 matched healthy control (HC) performed CMR on 3T scanner (Skyra, Siemens). NIHF was diagnosed by echocardiography, coronary artery angiogram and myocardial perfusion SPECT. Native T1 map was obtained by modified MOLLI 5-3 sequence and ECV was calculated 12 min. after GBCA 1.5 dose with 4-3-2 sequence on 4C view. Texture analysis was performed with LIFEx(www.lifexsoft.org). We also measured the wall thickness (WT) and outer diameter (OD) of LV.

Results: NIHF had larger OD of LV (78 +/- 16 mm) than the HC (57 +/- 6 mm) (P,0.001) while the WT had no difference (10.9 +/- 3.4 mm vs. 10.2 +/- 2.6 mm, p=0.41). Native T1 was significantly higher in NIHF patients (1310 +/- 48 ms) compared to HC (1208 +/- 72 ms) (p<0.001), while the ECV showed no difference (29 +/- 4.8% vs. 27 +/- 5%, p=0.30). The texture analysis of T1 and ECV maps showed no difference in the first-order textures and had significant difference in several second-order textures, such as GLRLM, GLZLM. There was inverse correlation of ECV and WT of LV in NIHF (r=-0.61, p=0.002).

Conclusions: In NIHF with preserved WT of LV, texture analysis of T1 and ECV maps showed difference in the mean value of native T1 and texture features, which is promising as a base for machine learning with future larger cohort.

Keywords: *Texture analysis; T1 maps; extracellular volume; heart failure; cardiovascular magnetic resonance*

¹ Thu Duc City Hospital,
Viet Nam

² Kaohsiung Veterans General
Hospital, Taiwan

INTRODUCTION

Non-ischemic heart failure is a widely prevalent disease characterized by myocardial dysfunction resulting from a variety of causes, some of which have yet to be fully defined. In ambulatory and hospitalized patients with clinically manifest heart failure primary cardiomyopathy is diagnosed in 2-15%, while in recent large scale therapeutic trials the proportion of patients with nonischemic heart failure ranged from 18-53% (1). Lack of accurate and noninvasive characterization of diffuse myocardial disease limits recognition of early cardiomyopathy and effective clinical management in NIHF. Endomyocardial biopsy is the suggested gold standard for detection and classification of myocardial tissue abnormalities, yet its invasiveness, low diagnostic yield, and paucity of proven consequential management pathways limit its widespread use in guiding clinical management (2). Recent studies have shown that T1- mapping techniques provide new insight into the quantification of fibrosis, of infiltration or scar and post-contrast myocardial T1 has been shown to significantly correlate with histological areas of fibrosis (3,4,5).

Texture analysis is a technique used for the quantification of image texture. Quantification of the intrinsic heterogeneity of different tissues and lesions is necessary as they are usually imperceptible to the human eye (6). In addition, texture can be quantified using different algorithms. To date, the TA of cardiovascular magnetic resonance (CMR) T1 and ECV maps have not been reported in non-ischemic heart failure.

We hypothesized that the extraction of texture of cardiac MRI images using T1 and ECV maps could find the textures that differ between pathological and normal myocardium, and this will be the basis for the future developing of machine learning.

MATERIALS AND METHODS

Study populations

This retrospective study included 23 NIHF (mean age = 48.1 years, 12 males), 25 matched healthy control (HC) (mean age = 48.1 years, 12 males) were recruited between March 2017 and december 2019. The diagnosis of NIHF was base on the clinical examination,

previous other investigation like echocardiography, coronary artery angiogram and myocardial perfusion SPECT, full the accepted criteria (7,8,9). Reduced LV ejection fraction compared with published refence ranges normalized for age and sex (10). Patients were excluded, if they had evidence of ischemic heart disease, defined as significant documented coronary artery disease, previous coronary revascularization, previous history of myocardial infarction, or evidence of ischemic type LGE, or inducible ischemia on stress testing.

Healthy controls without systemic illness or history of cardiovascular problems underwent 12 – lead electrocardiogram (ECG), echocardiography and CMR. All these examinations revealed no abnormalities. It was observed that the CMR had good image quality.

MRI acquisition

CMR was performed using 3T MRI machine (Skyra, Siemens, Germany) with 16 channel cardiac receiver coil. For all subjects, native and post -T1 mapping were performed with steady-state-free-precession single-breath-hold modified-Look-Locker inversion recovery (MOLLI) with (TR = 353.45 ms, TE = 1.08 ms, flip angle 35°, type 5-3) and (TR = 444.72 ms, TE = 1.18 ms, flip angle 35°, type 4-3-2) on 4C view. ECV was calculated 12 minutes after gadolinium-based contrast agent 1.5 dose (0.15 mmol/kg of Gadovist, Bayer, Germany) with 20 ml saline flushing, and using the following formula: $ECV = (1 - \text{hematocrit}) \times (\Delta R1_{\text{myocardium}} / \Delta R1_{\text{blood}})$, where R1 is (1/T1 pre-contrast-1/T1 post-contrast).

Texture analysis

Texture analysis which was a process that consists of six steps: MRI acquisition, ROI (region of interest), ROI preprocessing, feature extraction, feature selection, and classification, was performed with LIFEx (www.lifexsoft.org). Digital Imaging and Communication in Mdecine (DICOM) file of native T1 and post-T1 mapping was imported into LIFEx for further analysis. The margins of the myocardium were drawn carefully using a freehand region of interest (ROI) tool, avoiding the papillary muscle and the epicardial fat (figure 1) Grey-level normalization was performed by rescaling the threshold to minimize the brightness and contrast variation on TA. Seven

subsets of features including image shape, histogram, conventional, GLCM, GLRM, NGLDM, GLZLM, and were extracted with a total of 47 texture features. The texture subsets and corresponding features are summarized in table 1. Histogram and GLCM are commonly used texture parameters. Histogram reflects the frequency of a voxels' gray level in the image. The gray level histogram is the result of the statistics of a pixel on the image with a gray level, and the GLCM is the statistics of 2 pixels with a certain distance to maintain a certain gray level. The grey-level run length

matrix (GLRLM) gives the size of homogeneous runs for each grey level. This matrix is computed for the 13 different directions in 3D and for each of the 11 texture indices derived from this matrix, the 3D value is the average over the 13 directions in 3D. The element (i,j) of GLRLM corresponds to the number of homogeneous runs of j voxels with intensity i in an image and is called GLRLM thereafter. Similarly, The grey-level zone length matrix (GLZLM) [Thibault] provides information on the size of homogeneous zones for each grey-level in 3 dimensions (or 2D) (11)

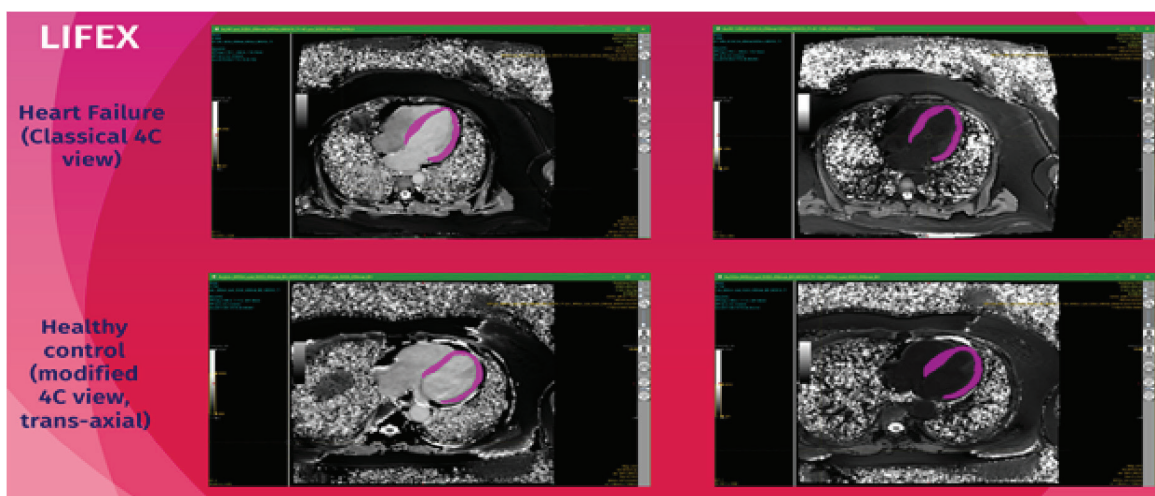


Figure 1. Texture feature analysis

Table 1. Texture subsets and corresponding features

| Order | Subset | Features |
|--------------|--------------|--|
| First Order | Shape | <input checked="" type="checkbox"/> SHAPE_Sphericity <input checked="" type="checkbox"/> SHAPE_Compacity <input checked="" type="checkbox"/> SHAPE_Volume_mL <input checked="" type="checkbox"/> SHAPE_Volume_vx |
| | Histogram | <input checked="" type="checkbox"/> HISTO_Skewness <input checked="" type="checkbox"/> HISTO_Kurtosis <input checked="" type="checkbox"/> HISTO_Entropy_log10 <input checked="" type="checkbox"/> HISTO_Entropy_log2 <input checked="" type="checkbox"/> HISTO_Energy |
| | Conventional | <input checked="" type="checkbox"/> CONV_SUV (min, mean, sd, max) <input checked="" type="checkbox"/> CONV_SUVpeak 0.5mL <input checked="" type="checkbox"/> CONV_SUVpeak 1mL <input checked="" type="checkbox"/> CONV_TLG |
| Second Order | GLCM | vx : distance with neighbours <input checked="" type="checkbox"/> GLOM_Homogeneity <input checked="" type="checkbox"/> GLOM_Energy <input checked="" type="checkbox"/> GLOM_Contrast <input checked="" type="checkbox"/> GLOM_Correlation <input checked="" type="checkbox"/> GLOM_Entropy <input checked="" type="checkbox"/> GLOM_Dissimilarity |
| | GLRM | <input checked="" type="checkbox"/> GLRM_SRE <input checked="" type="checkbox"/> GLRM_LRE <input checked="" type="checkbox"/> GLRM_LGRE <input checked="" type="checkbox"/> GLRM_HGRE <input checked="" type="checkbox"/> GLRM_SRLGE <input checked="" type="checkbox"/> GLRM_SRHGE <input checked="" type="checkbox"/> GLRM_LRLGE <input checked="" type="checkbox"/> GLRM_LRHGE <input checked="" type="checkbox"/> GLRM_GLNU <input checked="" type="checkbox"/> GLRM_RLNU <input checked="" type="checkbox"/> GLRM_RP |
| | NGLDM | <input checked="" type="checkbox"/> NGLDM_Coarseness <input checked="" type="checkbox"/> NGLDM_Contrast <input checked="" type="checkbox"/> NGLDM_Busyness |
| | GLZLM | <input checked="" type="checkbox"/> GLZLM_SRE <input checked="" type="checkbox"/> GLZLM_LZE <input checked="" type="checkbox"/> GLZLM_LGZE <input checked="" type="checkbox"/> GLZLM_HGZE <input checked="" type="checkbox"/> GLZLM_SZLGE <input checked="" type="checkbox"/> GLZLM_SZHGE <input checked="" type="checkbox"/> GLZLM_LZLGE <input checked="" type="checkbox"/> GLZLM_LZHGE <input checked="" type="checkbox"/> GLZLM_GLNU <input checked="" type="checkbox"/> GLZLM_ZLNU <input checked="" type="checkbox"/> GLZLM_ZP |

4C plane with auto-contouring of the endocardial and epicardial borders for automatic quantification of wall thickness (WT) and outer diameter (OD) of LV were calculated using Oxiris software. The borders and the contours were manually edited as needed. LV myocardial thickness was measured as the perpendicular distance

between the endocardial and epicardial borders of LV end-diastolic. Measurements of LV internal end-diastolic diameter (LVIDD) and septal and free end-diastolic wall diastolic thicknesses (IVSd and FWd). LV external end-diastolic diameter (LVEDD) was calculated per patient as LVEDD=LVIDD+IVSd+FWd.

Statistical analysis

Continuous variables are presented as means ± standard deviations. The texture features derived from the T1 mapping of the heart in patient with NIHF and HC were compared. Comparisons between two groups

were analyzed using the independent t-test. Correlation between ECV and WT was assessed using Pearson's test. A p-value of <0.05 was considered statistically significant. All the statistical analyses were performed using SPSS (V22, SPSS, Chicago, IL)

RESULTS

LV thickness and outer wall diameter

No significant differences were found in thickness of IVS and FW between patients with INHF and control patients (p =0.424, p= 0.438). However, In the INHF group, LV outer wall diameter was significantly higher than that of HC (p<0.001); The values are summarized in table 2.

Table 2. LV thickness and outer wall diameter

| | | N | MEAN | SD | SIG |
|----------------------|----|----------|-------------|-----------|------------|
| IVS thickness_ D_ cm | HC | 25 | 1.023 | 0.256 | 0.418 |
| | HF | 23 | 1.094 | 0,343 | 0.424 |
| FW thickness_ D_ cm | HC | 25 | 0.732 | 0.365 | 0.437 |
| | HF | 23 | 0.866 | 0,374 | 0.438 |
| LV ow_ D_ cm | HC | 25 | 5.709 | 0.569 | 0.000 |
| | HF | 23 | 7.869 | 1,616 | 0.000 |

Native T1 map value and ECV

NIHF patients had greater T1 values than normal (1310±48 vs. 1208±72 ms, p<0.001) while the mean values of ECV of IVS and FW were not significantly different between both groups

Table 3. native T1 map value and ECV

| | | N | MEAN | SD | SIG |
|-------------------|----|----------|-------------|-----------|------------|
| Native T1 map_IVS | HC | 25 | 1208.440 | 72.285 | 0.000 |
| | HF | 23 | 1310.360 | 48.112 | 0.000 |
| ECV_IVS | HC | 25 | 0.270 | 0.050 | 0.304 |
| | HF | 23 | 0.290 | 0.048 | 0.303 |
| ECV_FW | HC | 25 | 0.260 | 0.040 | 0.587 |
| | HF | 23 | 0.270 | 0.047 | 0.589 |

TA of native T1 map - First-order textures

The results of the T test in table 4 showed that most of the histogram features had no significant variation between non-ischemic heart failure patients and healthy controls (p>0.05)

Table 4. The first-order texture from histogram

| | | N | ME AN | SD | SIG |
|--------------------------------|----|----------|--------------|-----------|------------|
| Pre Diast_HISTO_Skewness | HC | 25 | 0.602 | 0.750 | 0.580 |
| | HF | 23 | 0.479 | 0.782 | 0.581 |
| Pre Diast_HISTO_Kurtosis | HC | 25 | 5.122 | 2.299 | 0.846 |
| | HF | 23 | 4.995 | 2.214 | 0.846 |
| Pre Diast_HISTO_ExcessKurtosis | HC | 25 | 2.122 | 2.299 | 0.846 |
| | HF | 23 | 1.995 | 2.214 | 0.846 |
| Pre Diast_HISTO_Entropy_log10 | HC | 25 | 1.468 | 0.111 | 0.289 |
| | HF | 23 | 1.437 | 0.084 | 0.284 |
| Pre Diast_HISTO_Entropy_log2 | HC | 25 | 4.876 | 0.370 | 0.289 |
| | HF | 23 | 4.774 | 0.280 | 0.284 |
| Pre Diast_HISTO_Energy | HC | 25 | 0.044 | 0.013 | 0.540 |
| | HF | 23 | 0.047 | 0.011 | 0.537 |

TA of native T1 map – Second-order textures

The several second-order textures like the grey-level run length matrix, the grey level zone length matrix showed significant differences (p<0.05)

Table 5. some texture features from second-order textures

| | | N | MEAN | SD | SIG |
|------------------------|----|----------|-------------|-----------|------------|
| Pre Diast_GLRLM_LGRE | HC | 25 | 0.006 | 0.012 | 0.030 |
| | HF | 23 | 0.001 | 0.001 | 0.028 |
| Pre Diast_GLRLM_HGRE | HC | 25 | 1 175.960 | 410.590 | 0.000 |
| | HF | 23 | 1616.442 | 396.286 | 0.000 |
| Pre Diast_GLRLM_SRIGE | HC | 25 | 0.004 | 0.006 | 0.016 |
| | HF | 23 | 0,001 | 0.001 | 0.015 |
| Pre Diast_<GLRLM_SRHGE | HC | 25 | 1114.234 | 396.508 | 0.001 |
| | HF | 23 | 1523,583 | 395.429 | 0.001 |
| Pre Diast_GLRLM_LRHGE | HC | 25 | 1480,519 | 477.646 | 0.000 |
| | HF | 23 | 2134,851 | 482.152 | 0.000 |
| Pre Diast_GLRLM_RLNU | HC | 25 | 733.563 | 247.254 | 0.021 |
| | HF | 23 | 585.954 | 168.7 1S | 0.019 |

| | | N | MEAN | SD | SIG |
|------------------------|-----|----|-------------|----------|-------|
| Pre Diast_GLZLM_LGZE | HC | 25 | 0.003 | 0.005 | 0.013 |
| | HF | 23 | 0.001 | 0.001 | 0.017 |
| Pre Diast_GLZLM_I-IGZE | HC | 25 | 1222.093 | 414.055 | 0.001 |
| | H F | 23 | 1 64 1 .G81 | 384.752 | 0.001 |
| Prc Diast_GLZLM_SZLGE | HC | 25 | 0.002 | 0.003 | 0.023 |
| | HF | 23 | 0.001 | 0.001 | 0.022 |
| Pre Diast_GLZLM_SZHGE | HC | 25 | 1022.867 | 364.833 | 0.002 |
| | HF | 23 | 1376.036 | 373.932 | 0.002 |
| Pre Diast_GLZLM_LZHGE | HC | 25 | 3 152.461 | 861.726 | 0.000 |
| | HF | 23 | 5943.264 | 3098.747 | 0.000 |
| Pre Diast_GLZLM_ZLNU | HO | 25 | 394.972 | 126.505 | 0.022 |
| | HF | 23 | 323.820 | 72.025 | 0.020 |

Non-ischemic heart failure - LV thickness and ECV

When analyzed in the heart failure group, we found that LV thickness inverse to ECV of IVS (r=-0.61, p=0.002).

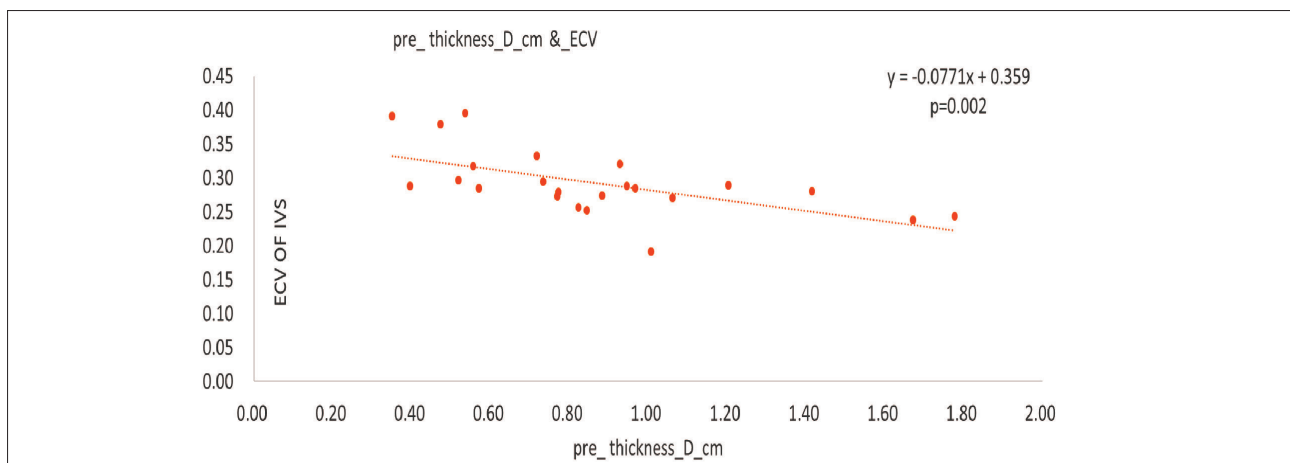


Figure 2. Relationship between LV thickness and ECV

DISCUSSION

In non ischaemic cardiomyopathy, ventricular dysfunction is a consequence of myocardial related to including haemodynamic pathology, infection, immunologic abnormalities, toxic injury, or genetic factors. Any of the cardiac pathology causing myocardial dysfunction results in abnormal myocyte growth, with a resultant cascade of gen activation stimulating cardiac remodeling. The hallmarks of cardiac remodeling are

myocardial cell hypertrophy and cardiac dilation with increased interstitial matrix formation. In late stage, the pathologic progress is characterized by myocytolysis, a disruption of sarcomeres. In the chronic phase, some components increase and cause myocyte death, creating perivascular fibrosis within intramuscular vessels. This process causes fibrillary collagen to fill the place of dead myocytes. Ultimately, the disruption of mechanical power by the damaged myocytes becomes

detrimental, and the left ventricular wall becomes thinner and dilated (12) In the present study, LV thickness of NIHF was similar to that of HC. This result suggest that our patient group had not yet reached the stage of dilated cardiomyopathy. However, our study found a larger outer diameter of heart failure patients. This suggests that this parameter is more valuable in NIHF.

Native T1 map measures a composite signal from myocytes and interstitium. Also, it provides new insight into the quantification of fibrosis, infiltration or scar. Our study demonstrated that the mean T1 values were significantly differences between patients and normal groups while, ECV values were similarities in both groups. Moreover, it found that TA of native T1 images, especially the second-order features is feasible for finding the difference of pathological and normal myocardium in NIHF. This study also has similar results with some studies on native T1 mapping application to distinguish some cardiomyopathies such as dilated cardiomyopathy, hypertensive disease, hypertrophic cardiomyopathy (author Ulf Neisius et al (13), author Shao et al (14)). The histogram and GLCM are two of the most commonly used texture parameters like the two studies above while in the present study showed

that TA of T1 mapping had significant difference in several second-order textures, such as GLRLM, GLZLM, composite GLRM_LGRE, GLRLM_HGRE, GLRLM_SRLGE, GLRLM_SRHGE, GLRLM_SRHGE, GLRLM_LRHGE, GLRLM_RLNU, GLZLM_LGZE, GLZLM_HGZE, GLZLM_SZLGE, GLZLM_SZHGE, GLZLM_LZHGE, GLZLM_ZLNU. In comparison to first order features, where a lot of the spatial information was lost through the transformation of gray levels into counts in the histogram, GLRLM, and GLZLM features contain more information about the distribution of gray values since they account for the location of each voxel with regard to the neighboring voxels (15,16).

The present study had several limitations. First, the small sample size restricted the subgroup analysis of NIHF. Second, for the software property, we analyzed only one 4C view image. Two-dimensional texture features may produce a selection bias.

CONCLUSION

In NIHF with preserved WT of LV, texture analysis of T1 and ECV maps showed difference in the mean value of native T1 and texture features, which is promising as a base for machine learning with future larger cohort

REFERENCES

1. Follath et al. 'Nonischemic heart failure: epidemiology, pathophysiology and progression of disease', *J Cardiovasc Pharmacol.* 1999 Jun; 33 Suppl 3:S31-5
2. L.T. Cooper, K.L. Baughman, A.M. Feldman, et al., 'The role of endomyocardial biopsy in the management of cardiac disease: a scientific statement from the American Heart Association, the American College of Cardiology, and the European Society of Cardiology. Endorsed by the Heart Failure Society of America and the Heart Failure Association of the European Society of Cardiology', *J Am Coll Cardiol*, 50 (2007), pp.1914-1931
3. Iles L, Pfluger H, Phrommintikul A, Cherayath J, Aksit P, Gupta SN, Kaye DM, Taylor AJ, 'Evaluation of diffuse myocardial fibrosis in heart failure with cardiac magnetic resonance contrast-enhanced T1 mapping', *J Am Coll Cardiol.* 2008 Nov 4; 52(19):1574-80.
4. Peter P Swoboda and al. 'Role of T1 Mapping in Inherited Cardiomyopathies', *Eur Cardiol.* 2016 Dec; 11(2): 96–101.
5. Ordovas KG, Higgins CB., 'Delayed contrast enhancement on MR images of myocardium: past, present, future', *Radiology* 2011;261:358–74.
6. Andres Larroza, Vicente Bodi and David Moratal, 'Texture analysis in Magnetic Resonance Imaging review and considerations for future application', 2016

-
7. World Health Organization. International Classification of Diseases (ICD). Available at: <http://www.who.int/classifications/icd/en/>. Accessed August 3, 2015.
 8. P. Elliott, B. Andersson, E. Arbustini, et al., 'Classification of the cardiomyopathies: a position statement from the European Society of Cardiology Working Group on Myocardial and Pericardial Diseases', *Eur Heart J*, 29 (2008), pp. 270-276.
 9. E. Arbustini, N. Narula, L. Tavazzi, et al., 'The MOGE(S) classification of cardiomyopathy for clinicians', *J Am Coll Cardiol*, 64 (2014), pp. 304.
 10. A. Gulati, A. Jabbour, T.F. Ismail, et al., 'Association of fibrosis with mortality and sudden cardiac death in patients with nonischemic dilated cardiomyopathy', *JAMA*, 309 (2013), pp. 896-908
 11. F.Orlhac, C.Nioche, I. Buvat, 'texture – user guide Local Image Features Extraction – LIFEx', LIFEx version 4.nn (2020)
 12. Kaan Kirali, Tanil Ozer and Mustafa Mert Ozgur, 'Pathophysiology in heart failure', 2017.
 13. Ulf Neisius, Hossam El-Rewaidy, Shiro Nakamori, Jennifer Rodriguez, Warren J. Manning, and Reza Nezafat, 'Radiomic Analysis of Myocardial Native T1 Imaging Discriminates between Hypertensive heart disease and hypertrophic cardiomyopathy', *J Am Coll Cardiol Img*. 2019 oct, 12 (10) 1946-1954.
 14. Shao, Xiao-Ning MS^a; Sun, Ying-Jie MS^b; Xiao, Kun-Tao MS^c; Zhang, Yong MD^a; Zhang, Wen-Bo MS^a; Kou, Zhi-Feng MD^d; Cheng, Jing-Liang MD, 'Texture analysis of magnetic resonance T1 mapping with dilated cardiomyopathy, A machine learning approach', *Medicine*: September 2018 – volume 97- issue 37- pe12246
 15. Anton S Becker, Soleen Ghafoor, Magda Marcon, Jose A Perucho, Moritz C Wurnig, Matthias W Wagner, Pek-Lan Khong, Elaine YP Lee, and Andreas Boss, 'MRI texture features may predict differentiation and nodal stage of cervical cancer: a pilot study', *Acta Radiol Open*. 2017 oct; 6 (10).
 16. Ayushman Ramola, Amit Kumar Shakyra, Dai Van Pham, 'Study of statistical methods for texture analysis and their modern evolutions' *Engineering Reports*, March 2020- volume 2, issue 4 e12149

Correspondent: Chau Thi Ngoc Anh. Email: dr.chausingocanh@gmail.com

Received: 20/10/2021. Assessed: 26/10/2021. Reviewed: 03/11/2021. Accepted: 05/11/2021